Biogenesis of the Protein Storage Vacuole Crystalloid

Liwen Jiang,*‡ Thomas E. Phillips,§ Sally W. Rogers,* and John C. Rogers*

*Institute of Biological Chemistry, Washington State University, Pullman, Washington 99164-6340; ‡Department of Biology, The Chinese University of Hong Kong, Shatin, New Territories, Hong Kong, China; and §Division of Biological Sciences, University of Missouri, Columbia, Missouri 65211

Abstract. We identify new organelles associated with the vacuolar system in plant cells. These organelles are defined biochemically by their internal content of three integral membrane proteins: a chimeric reporter protein that moves there directly from the ER; a specific tonoplast intrinsic protein; and a novel receptor-like RING-H2 protein that traffics through the Golgi apparatus. Highly conserved homologues of the latter are expressed in animal cells. In a developmentally regulated manner, the organelles are taken up into vacuoles where, in seed protein storage vacuoles, they form a membrane-containing crystalloid. The uptake and preservation of the contents of these organelles in vacuoles represents a unique mechanism for compartmentalization of protein and lipid for storage.

Key words: integral membrane protein • storage protein • prevacuolar compartment • autophagy • RING-H2

Introduction

Plant cells compartmentalize proteins in the secretory pathway for storage (Okita and Rogers, 1996). Proteins stored in seeds comprise the major food source for humanity (Müntz, 1998), and, in the seeds of dicotyledonous plants, storage occurs exclusively in vacuoles (Herman and Larkins, 1999). Protein storage vacuoles (PSVs),[1] previously termed protein bodies (Lott, 1980; Weber and Neumann, 1980), are the storage organelles in seeds. Their surrounding tonoplast membrane is biochemically distinguished from that of lytic or digestive vacuoles by the presence together of two tonoplast intrinsic proteins (TIPs), α- and δ-TIP (Hoh et al., 1995; Paris et al., 1996; Jauh et al., 1999). Consistent with the concept that PSVs and lytic vacuoles are distinct organelles, in developing pea cotyledons, soluble proteins are carried to PSVs in dense vesicles (Hinz et al., 1999); these are morphologically and biochemically distinct from clathrin-coated vesicles that traffic in the lytic vacuole pathway (Robinson et al., 1998a).

In contrast to the lytic vacuole pathway, where a probable sorting receptor has been identified (Kirsch et al., 1994; Paris et al., 1997) and a prevacuolar compartment has been defined morphologically (Paris et al., 1997) and functionally (Jiang and Rogers, 1998), less is known of mechanisms for sorting into dense vesicles and of intermediate compartments on the pathways to the PSV. Physical aggregation may serve as a sorting mechanism (Neuhaus and Rogers, 1998), but there are suggestions in the literature that some type of sorting receptor may be involved. It has been observed that overexpression of soluble proteins that traffic in an equivalent of the dense vesicle pathway results in their secretion (Neuhaus et al., 1994; Frigerio et al., 1998).

Two different structures with features consistent with what would be expected for a PSV prevacuolar compartment have been identified. In developing pea seeds, multivesicular bodies ranging in size from ~0.5 to several micrometers that contain storage proteins have been postulated as prevacuolar organelles (Robinson et al., 1998a,b). In contrast, in developing pumpkin and castor bean seeds, precursor-accumulating vesicles, <0.5 μm in size, are comprised of a central osmiophilic core that contains storage proteins and derives directly from the ER (Hara-Nishimura et al., 1998). Additionally, these vesicles contain a peripheral translucent layer with internal vesicles where glycoproteins with Golgi-mediated complex modifications to asparagine-linked oligosaccharides are localized (Hara-Nishimura et al., 1998). The latter observation indicates that, although precursor-accumulating vesicles originally bud from the ER, they may also serve as a destination for vesicular traffic from the Golgi apparatus. The concept in both systems is that the multivesicular

Address correspondence to John C. Rogers, Institute of Biological Chemistry, Washington State University, Pullman, WA 99164-6340. Tel.: (509) 335-2773. Fax: (509) 335-7643. E-mail: bcjroger@wsu.edu

[1]*Abbreviations used in this paper:* CM, cell membrane fraction; CS, cell soluble fraction; CT, cytoplasmic tail; DIP, dark intrinsic protein; EST, expressed sequence tag; GUS, *Escherichia coli* β-glucuronidase; PSV, protein storage vacuole; RMR protein, receptor homology region-transmembrane domain-Ring H2 motif; TIP, tonoplast intrinsic protein; TMD, transmembrane domain.

bodies (Robinson et al., 1998a) and precursor-accumulating vesicles (Hara-Nishimura et al., 1998) fuse with developing PSVs to deliver their cargo.

Consideration of the plant PSV system is complicated by the fact that PSVs in most seeds are complex organelles with three distinct components: (1) a matrix that contains most of the soluble storage proteins; (2) a crystalloid composed of unknown proteins organized in a lattice structure; and (3) globoid cavities that may contain phytic acid or oxalate crystals (Lott, 1980; Spitzer and Lott, 1980; Weber and Neumann, 1980). In contrast, PSVs in legume seeds (including peas) lack crystalloid (Lott, 1980; Weber and Neumann, 1980). The matrix and crystalloid appear to be destinations for different types of proteins. When expressed in transgenic tobacco seeds, the bean seed storage proteins, phaseolin and phytohemagglutinin, were localized to the PSV matrix (Greenwood and Chrispeels, 1985; Hoffman et al., 1987; Sturm and Chrispeels, 1988), whereas the maize 15-kD zein was localized to the PSV crystalloid (Hoffman et al., 1987). The origin of the crystalloid and its functional implications are not known.

In addition to the results from precursor-accumulating vesicle studies (Hara-Nishimura et al., 1998), the results from studies of traffic of chimeric integral membrane proteins to vacuoles in tobacco suspension culture protoplasts indicated that some membrane components of organelles in the PSV pathway may derive directly from the ER (Jiang and Rogers, 1998). A chimeric protein comprised of a lumenal reporter domain attached to only the transmembrane domain (TMD) of the probable vacuolar sorting receptor BP-80 trafficked from the ER through the Golgi apparatus to the lytic vacuole pathway. In contrast, attachment of the 15–amino acid COOH-terminal cytoplasmic tail (CT) of the PSV-specific α-TIP caused that reporter (now designated the α-TIP CT reporter or Re-F-B-α) to move directly from the ER, bypassing the Golgi apparatus, to a second type of vacuole. This vacuole was also the destination of intact α-TIP, when it and the chimeric reporter were expressed together, and, therefore, was considered to be a PSV equivalent in the tobacco protoplasts (Jiang and Rogers, 1998).

Here, we have used transgenic tobacco plants expressing the α-TIP CT reporter to dissect more details of this ER to PSV pathway. We show that the reporter protein localizes to small organelles in root tip cells and developing seeds that are marked by the presence of a unique tonoplast intrinsic protein termed dark intrinsic protein (for DIP; Culianez-Macia and Martin, 1993) and are predominantly located in the cytoplasm. As seed development proceeds, these organelles are taken up by PSVs and aggregate such that they form the crystalloid in mature seeds. These organelles also represent an intermediate for vesicular traffic from the Golgi apparatus because they abundantly accumulate a unique receptor-like protein of the ReMembR-H2 (RMR) protein family that acquires Golgi-specific asparagine-linked oligosaccharide modifications. The structure of RMR proteins and their pattern of secretory pathway traffic indicate that they may assist in protein sorting into a vesicle pathway leading to the PSV, or may function to assemble other proteins within the crystalloid matrix.

Materials and Methods

General methods for construction of recombinant plasmids, screening of cDNA libraries and characterization of cloned inserts, transient expression of recombinant proteins in tobacco suspension culture cells, and preparation and characterization of antibodies have been previously described (Paris et al., 1997; Rogers et al., 1997; Jiang and Rogers, 1998)

Cloning of RMR Protein cDNAs

Two *Arabidopsis* expressed sequence tag (EST) sequences (these data are available from GenBank/EMBL/DDBJ under accession No. Z35151 and Z34589) were identified from BLAST searches (http://www.ncbi.nlm.nih.gov/) using the NH_2-terminal 400–amino acid sequence of VSR_{At-2} (Paris et al., 1997) as a query. The corresponding plasmids were obtained from the *Arabidopsis* Biological Resource Center (http://aims.cps.msu.edu/aims) and used to screen an *Arabidopsis* cDNA library provided by Dr. John Walker (University of Missouri, Columbia, MO; Paris et al., 1997). The cDNA inserts from clones JR700, corresponding to Z34589, and JR702, corresponding to Z35151, were sequenced on both strands (Paris et al., 1997). These sequences have been submitted to GenBank with accession numbers AF218807 and AF218808, respectively.

Agrobacterium-mediated Transformation and Generation of Transgenic Tobacco Plants

Plasmid PLJ-4 (Jiang et al., 1995) was used as a basis for constructing a transformation vector. The coding sequence for the Re-F-B-α reporter protein was inserted into PLJ-4 as a HindIII-SacI fragment to give construct 650. Plasmids PLJ-4 and 650 were separately transferred from *Escherichia coli* HB101 to the *Agrobacterium* strain LBA 4404 by triparental mating as previously described (Jiang et al., 1995). Transformation and regeneration of kanamycin-resistant transgenic tobacco plantlets were performed as previously described (Jiang et al., 1995). Transgenic plantlets were either maintained in a magenta box by transferring shoots to new media, or transferred to the greenhouse and grown to maturity for seed collection. The stages of seed development were estimated by tagging flowers at the time of anthesis just as the petals opened and began to turn pink.

Antibodies

A recombinant protein representing the lumenal portion (NT) of the JR702 protein (residues 17–155) with six His residues at the COOH terminus was expressed in *E. coli*, purified as described (Rogers et al., 1997), and used for immunization of a rabbit. A synthetic peptide, acetyl-DART-STGEPPASESTP-amide corresponding to residues 272–287 of JR702, in its cytoplasmic tail (CT), was synthesized by Alpha Diagnostic International, and also used for immunization of a rabbit. These antibodies were affinity-purified (Rogers et al., 1997) before use. Preparation of affinity-purified antialeurain antibodies (Jiang and Rogers, 1998) and antibodies specific for the COOH-terminal cytoplasmic tail of four tonoplast intrinsic proteins (Rogers et al., 1997; Jauh et al., 1999) have been described. To detect α-TIP, we used the Mab38A mouse mAb (Næsted et al., 2000). To reduce possible cross-reactivity with tobacco proteins, acetone powder prepared from tobacco tissues was used to absorb the antialeurain antibodies before their use in immunofluorescence. The sources and use of the anti-FLAG monoclonal and antiplant complex glycan (Jiang and Rogers, 1998), and anti–mung bean vacuolar pyrophosphatase (Jauh et al., 1999) antibodies have been described. Antisera to tobacco class I vacuolar chitinase and to β-1,3-glucanase were provided by Dr. F. Meins (Friedrich Miescher Institute, Basel, Switzerland). Affinity-purified fluorochrome-tagged secondary antibodies were purchased from Jackson ImmunoResearch Laboratories. The JIM84 rat mAb directed against Lewis a–containing N-glycans (Fitchette et al., 1999) was provided by Dr. C. Hawes (Oxford Brookes University, Oxford, UK).

Transient Expression

The Re-F-R-R reporter protein construct contains the transmembrane domain and cytoplasmic tail from JR702 fused to the mutated proaleurain-FLAG linker sequences from construct 491 (Jiang and Rogers, 1998). To prepare the construct, two oligonucleotides were designed and used to generate PCR fragments. The 5′ primer contained an EcoRI site, followed by the FLAG sequence and the coding sequence for 24 amino acids from

JR702, beginning with residue 148. The 3′ primer contained a SacI site, followed by a stop codon and the last 24 JR702 codons, all in inverted order. JR702 DNA was used as a template for amplification. The resulting PCR fragment was digested with EcoRI and SacI and cloned into the EcoRI-SacI interval of construct 491 to yield construct 727. The fidelity of the construct was confirmed by restriction mapping and sequencing. Transient expression, cell labeling, subcellular fractionation, and immunoprecipitation were performed as previously described (Jiang and Rogers, 1998).

Confocal Immunofluorescence Studies

Fixation and preparation of cells from root tips and of tissue for paraffin-embedded sections, and their labeling and analysis by epifluorescence and confocal immunofluorescence have been described previously (Paris et al., 1996; Jauh et al., 1998, 1999). The extent of colocalization of two antibodies in confocal immunofluorescence images from both root tip cells and mature seed sections, and from protoplasts coexpressing α-TIP protein and a chimeric reporter protein in transient expression experiments, was quantitated as described previously (Jiang and Rogers, 1998). Controls to ascertain the specificity of double labeling experiments were performed as previously described (Jauh et al., 1999). Additionally, we confirmed that the labeling pattern for an antibody used individually matched the pattern obtained with the same antibody when used in double labeling experiments.

Electron Microscopy

Mature tomato and tobacco seeds, and immature developing tobacco seeds were scored to open the seed coat, and then fixed with 3.7% paraformaldehyde, embedded, sectioned, and studied by immunocytochemistry as previously described (Paris et al., 1997). For these studies, anti-DIP, anti–δ-TIP, and antialeurain antibodies were used at 20 μg/ml; anti-RMR NH_2-terminal and COOH-terminal antibodies were used in combination, each at 10 μg/ml. The primary antibodies were detected with 10 nm gold-labeled goat anti–rabbit IgG (Nanoprobes).

Purification of PSV Crystalloids

Pumpkin (*Cucurbita* sp., var. Small Sugar) seeds were purchased from the Lockhart Seed Company. Crystalloids were purified using modifications of the methods of Tully and Beevers (1976) and Hara-Nishimura et al. (1982). All procedures were performed at 4°C. 20 g of dry cotyledons were homogenized in 40 ml of glycerol in a Waring blender at high speed. The homogenate was poured through four layers of cheesecloth and centrifuged at 1,100 *g* for 10 min. PSVs were collected by centrifugation at 41,000 *g* for 20 min; the pellet was resuspended in 30 ml glycerol and again centrifuged at 41,000 *g* for 20 min. This pellet was identified as the PSV preparation. PSVs were disrupted by vigorously resuspending the pellet in 10 ml of 5 mM Tris-HCl, pH 8.5, 1 mM EDTA (TE buffer), and then fractionated by centrifugation onto a discontinuous step gradient prepared from 7 ml of 68% sucrose, 7 ml of 45% sucrose, and 7 ml of 30% sucrose (all in TE buffer) at 78,000 *g* for 2 h. The fraction above the 30% sucrose layer was identified as the matrix. The pellet was again resuspended in 10 ml TE buffer by vortexing and washed by centrifugation into a second discontinuous gradient comprised of 5 ml of 80% sucrose and 5 ml of 68% sucrose (both in TE buffer) at 78,000 *g* for 2 h. The pellet was resuspended in 5 ml TE and filtered through a layer of Miracloth (Calbiochem); the resulting suspension was identified as the crystalloid preparation. The protein was measured by the method of Bradford (1976) using BSA as a standard. The following total protein was recovered in each fraction: matrix, 350 mg; 30% sucrose surface, 54 mg; 30–45% interface, 46 mg; 45–68% interface, 72 mg; 68% surface (second gradient), 24 mg; and crystalloid, 12.8 mg.

Quantitation of Lipid

Samples of the crystalloid preparation and of the material collected at the surface of the 68% sucrose cushion from the second gradient were pelleted at 10,000 and 100,000 *g*, respectively. Each pellet was resuspended in 0.5 ml of ethanol/benzene 90:1 and dried thoroughly at 35°C under a stream of nitrogen. The fatty acyl components of lipids in the dried pellets were converted to fatty acid methyl esters and quantified by gas chromatography using an external standard as previously described (Browse et al., 1986).

Results

Expression of the αTIP CT Reporter (Re-F-B-α) in Transgenic Tobacco Plants

A direct ER to PSV-like compartment is marked by traffic of the Re-F-B-α reporter protein in tobacco suspension culture cells (Jiang and Rogers, 1998). To further characterize this pathway, we stably expressed this reporter protein (Fig. 1 A) in tobacco plants via *Agrobacterium*-mediated transformation (Jiang et al., 1995). Expression of the reporter protein in various independent transgenic plants was confirmed by immunoprecipitation using antialeurain/FLAG antibodies (Fig. 1 B). As shown in Fig. 1 B, membrane-associated (CM) full-length reporter protein was detected in extracts from five transgenic plants expressing the reporter protein (construct 650, lanes 7–16) but not from a control plant expressing *Escherichia coli* β-glucuronidase (GUS [Jefferson et al., 1987]; construct PLJ-4, lanes 5 and 6). The sizes of the reporter proteins detected in the transgenic plants were indistinguishable from that of the same reporter transiently expressed in the protoplast

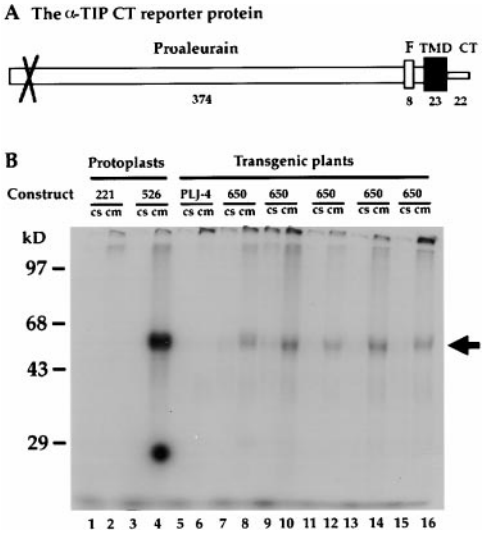

Figure 1. Expression of the α-TIP CT reporter protein (Re-F-B-α) in transgenic tobacco plants. (A) Schematic illustration of Re-F-B-α (Jiang and Rogers, 1998), which contains mutated proaleurain (open box with X indicating mutated vacuolar targeting sequence), a FLAG epitope (F, vertical gray rectangle), BP-80 transmembrane domain (TMD, black box), and the α-TIP COOH-terminal cytoplasmic tail (CT, thin gray rectangle). The numbers below the construct indicate the length, in amino acid residues, of each of the components. (B) Detection by immunoprecipitation of Re-F-B-α in transgenic plants. Root tips collected from several independently transformed transgenic plantlets (lanes 5–16; PLJ-4 = control plant expressing β-glucuronidase (GUS); 650 = plants expressing Re-F-B-α) were labeled with [^{35}S]methionine and cysteine for 3 h before cell-soluble (CS) and cell membrane (CM) fractions were collected. Each sample was double immunoprecipitated with antialeurain followed by anti-FLAG antibodies (Jiang and Rogers, 1998). Protein samples were separated by SDS-PAGE and detected by fluorography. As positive and negative controls, respectively, protoplasts expressing Re-F-B-α (construct 526) and GUS (construct 221) were labeled and fractionated as before. (arrow) Full-length Re-F-B-α.

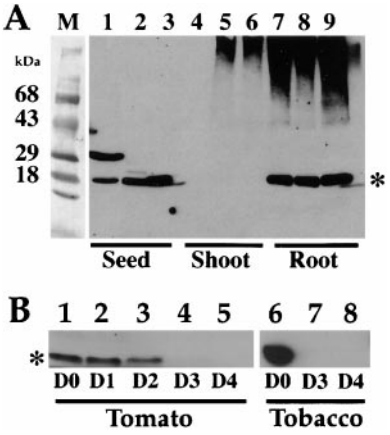

Figure 2. Characterization of anti-DIP antibodies. (A) Western blot detection of DIP in tissue extracts from three plant species. (lanes 1, 4, and 7) Extracts from snapdragon (*Antirrhinum majus*); (lanes 2, 5, and 8) extracts from tomato (*Lysopersicon esculentum*); and (lanes 3, 6, and 9) extracts from tobacco (*Nicotiana tabacum*). Asterisk indicates the position of DIP; and M indicates molecular mass markers in kilodaltons. (B) DIP protein in mature seeds disappeared upon germination. Mature tomato (lanes 1–5) and tobacco (lanes 6 and 7) seeds were imbibed in water for up to 4 d and protein extracts were prepared at the times indicated from day 0 (D0) to day 4 (D4). Asterisk indicates DIP.

system (lane 4). The reporter protein was much less abundant in the soluble (CS) fractions from the extracts, and was not present in the CM fraction from protoplasts expressing GUS (lane 2). Thus, Re-F-B-α was expressed properly in transgenic tobacco plants.

Characterization of Anti-DIP Antibodies

DIP is the fourth TIP isoform (Neuhaus and Rogers, 1998) for which we have prepared specific antibodies against using a peptide representing its COOH-terminal sequence (Jauh et al., 1998, 1999). DIP was originally identified as a cDNA from snapdragon (Culianez-Macia and Martin, 1993), but the DIP homologues of tobacco (GenBank X54855) and tomato (U95008) both contain a sequence identical to that of the peptide used for production of our anti-DIP antibodies. When tested by Western blot analysis, the anti-DIP antibodies identified a single protein band of ~22 kD (Fig. 2 A, asterisk) in extracts from seeds and root tips of snapdragon (lanes 1 and 7), tomato (lanes 2 and 8), and tobacco (lanes 3 and 9); this band was absent from all shoot extracts (lanes 4–6). Additionally, the antibodies detected a larger, ~30-kD band in the snapdragon seed extract, and a high molecular mass smear in each of the root tip extracts. Although ~22 kD is smaller than the expected size of 26–29 kD for a TIP, it is similar to that detected for an α-TIP homologue in pumpkin seeds (Inoue et al., 1995). In this case, the authors showed by NH_2-terminal sequence analysis that the smaller size was due to proteolytic cleavage within the first intralumenal loop. We have previously observed similar differences in sizes in TIPs from different sources detected on Western blots (Jauh et al., 1998, 1999). These results are consistent with previous studies showing that DIP and its tobacco homologue, TobRB7, were mainly expressed in seeds and roots (Yamamoto et al., 1991; Culianez-Macia and Martin, 1993). The close correspondence of results from three different plant species strongly argued that the antibodies were indeed specific for DIP protein. Additionally, when extracts were prepared from germinating tomato (Fig. 2 B, lanes 1–5) and tobacco (Fig. 2 B, lanes 6–8) seeds, the DIP protein band (asterisk) decreased upon the onset of germination and disappeared within 3 d of germination. These latter results indicated that accumulation of the DIP protein was tightly linked to storage processes in seeds.

Re-F-B-α Localized to A Unique Compartment Marked by the Tonoplast Intrinsic Protein, DIP

Root tip cells from transgenic tobacco plants were used for immunofluorescence studies to localize the Re-F-B-α reporter protein. Both our antialeurain and anti-FLAG antibodies gave little background staining of control cells, as shown in Fig. 3 A, 1 for anti-FLAG. In contrast, the anti-FLAG and antialeurain antibodies colocalized on round and elongated organelles with diameters of 1–2 μm in the cytoplasm of root tip cells from transgenic plants expressing the reporter protein (Fig. 3 A, 2, and Table I). Therefore, in subsequent experiments, we used either antibody to detect the reporter protein.

We screened a variety of antibodies that might label organelles associated with vacuoles (Jiang and Rogers, 1998; Jauh et al., 1999) in an attempt to characterize the organelle associated with the reporter protein. As shown in Fig. 3 A (3 and 4), only the anti-DIP antibodies colocalized with Re-F-B-α, as detected with antialeurain (Fig. 3 A, 3) or anti-FLAG (Fig. 3 A, 4) antibodies. These results were reproducible in studies of >200 cells. It should be noted that most DIP-positive organelles also contained the reporter protein, but occasionally, as shown in Fig. 3 A (4, arrowheads), organelles with a similar staining pattern

Figure 3. Re-F-B-α localized to a unique compartment marked by a specific tonoplast intrinsic protein, DIP. (A) Re-F-B-α and DIP colocalize in root tip cells of transgenic tobacco. Root tip cells collected from transgenic control plants expressing GUS (1), transgenic tobacco plants expressing Re-F-B-α (2 –6) or tomato plants (7), were fixed and double-labeled with two antibodies. Antialeurain and anti-FLAG antibodies were used to detect the reporter protein. The primary antibodies were detected with either Cy5-conjugated (pseudocolored green) or lissamine rhodamine-conjugated (pseudocolored red) antibodies. When green and red images are superimposed (both), colocalization of antibodies is indicated by a yellow color. Solid arrows in 2–4 indicate examples of organelles where the reporter protein and DIP are present together; arrowheads in 4 indicate a DIP organelle lacking staining for Re-F-B-α. (5) Images of cells labeled for DIP (red) and for the ER marker calnexin (green). The arrows indicate ER stained for calnexin that is separate from organelles stained for DIP (arrowhead). (6) Images of cells labeled for DIP (green) and the Golgi marker JIM84 (red). (7) Merged images of cells labeled with DIP (red) and V-PPase (green, left) or aleurain (red) and V-PPase (green, right) antibodies. (Open arrows) DIP organelles in cytosol; (closed arrows) DIP organelles closely associated with vacuole membranes; (arrowheads) DIP organelles in

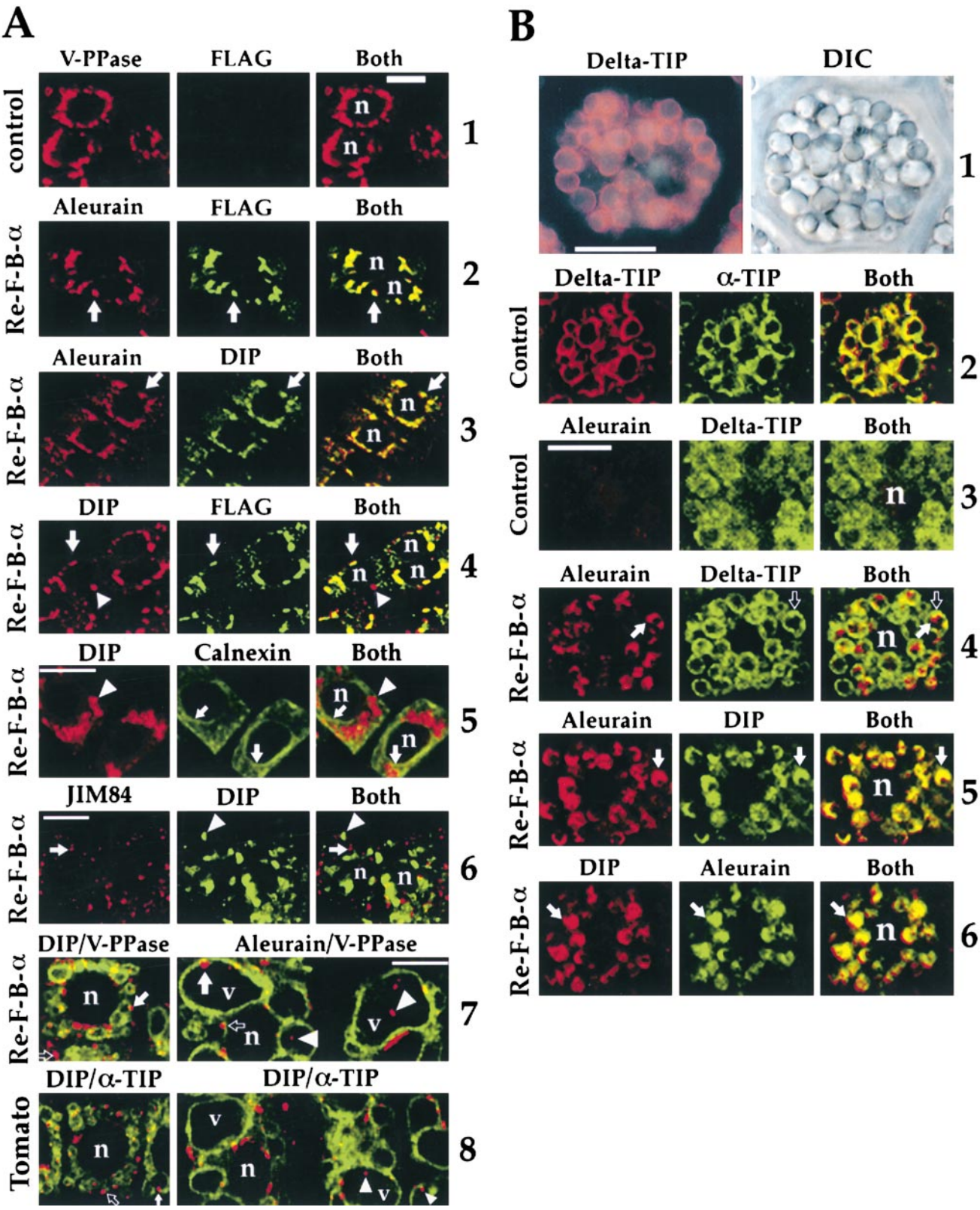

the lumen of vacuoles. (8) Merged images of tomato root tip cells labeled for DIP (red) and α-TIP (green); symbols as in 6. V-PPase, anti–vacuolar pyrophosphatase; n, nucleus; v, vacuole. (B) Re-F-B-α colocalized with DIP inside PSVs of mature transgenic tobacco seeds. Paraffin-embedded sections were prepared from mature transgenic tobacco seeds from control (1–3) and from Re-F-B-α–expressing plants (4–6) and double-labeled with two antibodies. The panels at the top (1) demonstrate PSVs in a single cell visualized by differential interference contrast (DIC, right), and by staining with anti–δ-TIP visualized with epifluorescence (left, red color), whereas the remaining panels present confocal immunofluorescence images. n, nucleus. Quantitation of the extent of colocalization for each pair of antibodies for relevant panels is presented in Table I. Bars, 10 μm.

Table I. Quantitation of Antibody Colocalization in Confocal Immunofluorescence Images

Antibodies compared	Percent colocalization	*n*
	mean ± SD	
A. Transgenic tobacco root tip cells expressing Re-F-B-α (Fig. 3 A)		
1. Aleurain:FLAG	93 ± 8	12
2. Aleurain:DIP	85 ± 10	10
3. DIP:FLAG	85 ± 10	11
4. DIP:calnexin	4 ± 3	10
B. Transgenic tobacco seeds expressing Re-F-B-α (Fig. 3 B)		
5. δ-TIP:α-TIP	93 ± 3	17
6. Aleurain:δ-TIP	8 ± 6	12
7. Aleurain:DIP	95 ± 5	10
8. DIP:aleurain	95 ± 7	10
9. JIM84:DIP	7 ± 4	23
C. Wild-type tobacco seeds (Fig. 5 A)		
10. DIP:δ-TIP	7 ± 6	10
11. Chitinase:DIP	12 ± 8	10
12. Chitinase:δ-TIP	13 ± 8	10
13. Chitinase:glucanase	95 ± 5	10
D. Tomato root tip cells (Fig. 8 A)		
14. RMR-NT:RMR-CT	98 ± 4	8
15. RMR-NT:DIP	96 ± 4	10
E. Tomato seeds (Fig. 8 B)		
16. δ-TIP:α	94 ± 3	10
17. RMR:δ-TIP	8 ± 9	8
18. DIP:δ-TIP	8 ± 3	8
19. RMR:DIP	93 ± 6	11

The Re-F-B-α reporter protein in transgenic tobacco cells was detected by antialeurain or anti-FLAG antibodies. The other antibodies were used to detect endogenous proteins in tobacco and tomato tissues. Quantitation of the extent of colocalization of two antibodies was performed as previously described (Jiang and Rogers, 1998). Percent colocalization is expressed as the mean ± SD for the (*n*) number of cells analyzed.

for DIP lacked detectable Re-F-B-α. When double label experiments using anti-DIP and anticalnexin antibodies, an ER marker (Jiang and Rogers, 1998), were performed, the two antibodies did not colocalize to any appreciable extent (Fig. 3 A, 5; Table I). Similarly, JIM84, a marker for Golgi apparatus (Fitchette et al., 1999) and anti-DIP, showed no colocalization (Fig. 3 A, 6, and Table I).

We used antivacuolar pyrophosphatase antibodies, a general marker for vacuole membranes (Jauh et al., 1999) to map the position of the DIP-positive organelles relative to vacuoles in root tip cells. As shown in Fig. 3 A (7, left), in smaller cells with relatively small vacuoles, the DIP-positive organelles appeared to be in the cytoplasm (open arrow) or closely apposed to vacuole membranes (solid arrow). In contrast, in larger cells with large vacuoles (Fig. 3 A, 7, right), the same organelles (here detected by their Re-F-B-α content) commonly appeared to be within the lumen of vacuoles (arrowheads). Serial optical sections of such cells confirmed that the organelles were within the vacuoles (data not presented). This localization is consistent with studies of PSVs in seeds (see below). Similar results were obtained with anti-DIP labeling of tomato root tip cells, where vacuole tonoplast was labeled with anti–α-TIP (Fig. 3 A, 8). We have not further classified the functional type of vacuoles in which the DIP-positive organelles were localized.

We reasoned, by virtue of their association with Re-F-B-α, that the DIP-positive organelles might be on a pathway to the PSV. Although PSVs are present in root tip cells (Paris et al., 1996; Jauh et al., 1999), they are best characterized in seeds. Therefore, we compared the localization of Re-F-B-α and DIP in mature seeds from transgenic tobacco plants. Consistent with previous studies of PSVs in pea seeds (Jauh et al., 1999), the tonoplast of tobacco seed PSVs was specifically labeled by both anti–δ-TIP (Fig. 3 B, 1; detected by epifluorescence in single labeling) and anti–α-TIP antibodies (Fig. 3 B, 2; confocal double labeling for α- and δ-TIP). As shown in Fig. 3 B, there was little background labeling by antialeurain antibodies in sections from seeds of control plants (Fig. 3 B, 3). In contrast, in cells from transgenic seeds, the reporter protein, as detected by antialeurain antibodies (Fig. 3 B, 4, red), was concentrated in structures mostly contained within PSVs marked by δ-TIP (green). Consistent with the results from the labeling of root tip cells, the reporter protein and DIP colocalized; the labeling results with the two antibodies were independent of the order in which the two primary antibodies were applied (Fig. 3 B, 5 and 6, and Table I).

Characterization of DIP Organelles

The finding that the DIP-positive structures appeared to be contained within PSVs was unexpected because previous studies have indicated that tonoplast intrinsic proteins, a family of which DIP is a member, are specific markers for the limiting membranes of plant cell vacuoles (Neuhaus and Rogers, 1998). However, the above results indicated that the DIP-positive structures were separate from the tonoplast membrane containing δ-TIP or α-TIP in PSVs. To further define the limits of the DIP-positive structures within tobacco seed PSVs, we compared the distribution of DIP to that of two tobacco proteins stored in PSVs, vacuolar chitinase, and glucanase (Neuhaus and Rogers, 1998). As shown in Fig. 4 A (1), which is consistent with results in Fig. 2, most DIP-positive structures (red) were contained within tonoplast marked by δ-TIP in PSVs (green). DIP-positive structures (green) also appeared to be surrounded by regions in PSVs where chitinase (red) was localized (Fig. 4 A, 2). However, the chitinase was contained within δ-TIP–labeled tonoplast, as indicated by the separation of chitinase (red, arrow) from δ-TIP (Fig. 4 A, 3, green, arrowhead). Glucanase and chitinase colocalized within PSVs (Fig. 4 A, 4, and Table I).

These results indicated that glucanase and chitinase were present in a space between the PSV tonoplast and the DIP-positive structures. We used electron microscopy immunocytochemistry to resolve the nature of these compartments. As shown in Fig. 4 B (1), anti–δ-TIP labeled the surrounding tonoplast of PSVs (arrow), whereas anti-DIP (Fig. 4 B, 2) heavily labeled the PSV crystalloid. When transgenic seeds from plants expressing the Re-F-B-α reporter protein were similarly studied using antialeurain antibodies, specific labeling of the crystalloid was also observed (Fig. 4 B, 3). These results are fully consistent with the immunofluorescence studies that demonstrated colocalization of DIP and Re-F-B-α; we also infer from these

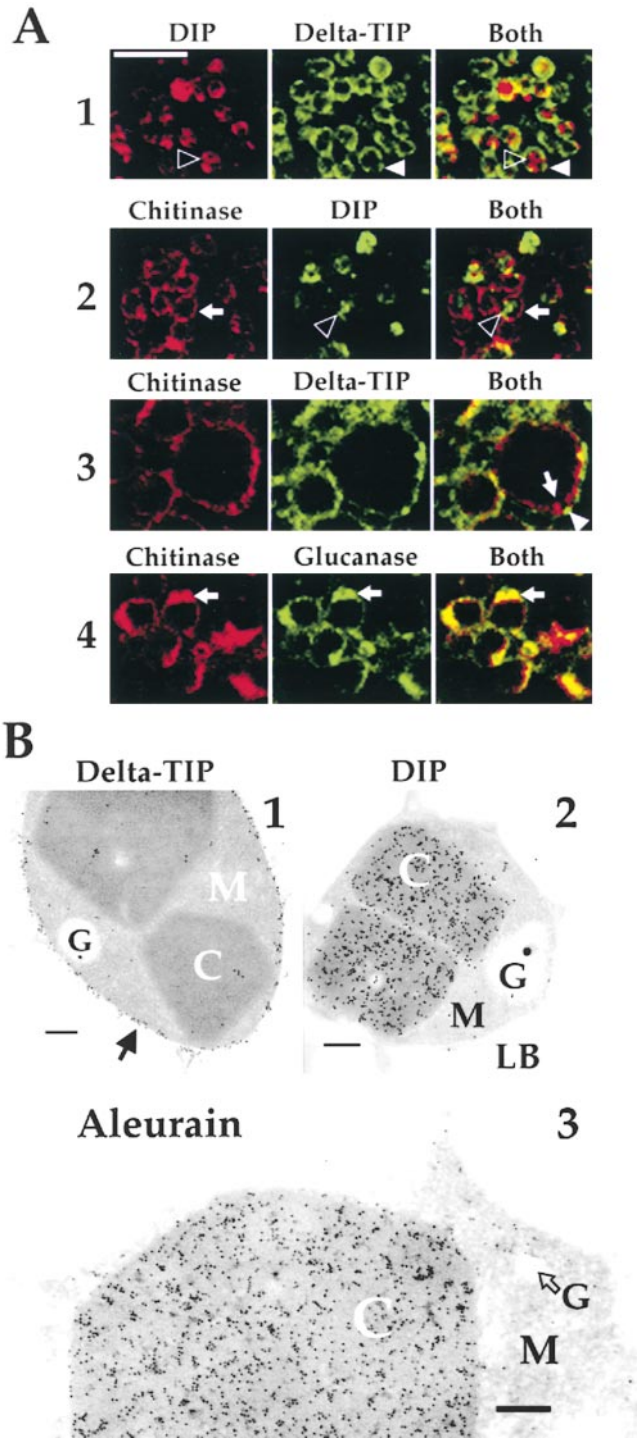

Figure 4. Characterization of DIP-positive structures in PSVs. (A) Confocal immunolocalization of DIP in relation to other PSV markers in mature tobacco seeds. Legends above each panel indicate antibodies used to label cells. (1) Organelle stained for DIP (open arrowhead) within PSV stained for δ-TIP (closed arrowhead); and (2) staining for chitinase (solid arrow) around the organelle stained for DIP (open arrowhead). (3) Staining for chitinase (arrow) inside a membrane stained for δ-TIP (arrowhead); and (4) staining for chitinase and glucanase colocalize (arrow). Quantitation of the extent of colocalization for each pair of antibodies is presented in Table I. (B) Immuno-EM localization of DIP (1), δ-TIP (2) (both from control plants), and aleurain from a transgenic plant expressing Re-F-B-α (3) in PSVs of mature tobacco seeds. C, crystalloid; M, matrix; LB, lipid body; G, globoid cavity. The PSV shown in 3 is from an endosperm cell and, thus, is larger than those from the embryo cells shown in 1 and 2. Bars: (A) 10 μm; (B) 200 nm.

results that glucanase and chitinase would be localized in the PSV matrix.

DIP Organelles Are External to the PSV in Developing Tobacco Seeds

Both DIP and Re-F-B-α are integral membrane proteins. Their specific localization to the PSV crystalloid defines it as a membrane-containing compartment separate from PSV tonoplast. We asked how crystalloid membrane could enter the PSV, and what relationship crystalloid had to the small DIP- and reporter-containing organelles outside of vacuoles in root tip cells. Answers to these questions came from studies of developing tobacco seeds.

DIP organelles (red, arrow), similar in size to those observed in root tip cells (Fig. 3), were mainly separated from PSVs marked by δ-TIP (green, arrowhead) during early seed development (10 d after pollination; Fig. 5 A, 1); similar results were obtained with anti-DIP and anti–α-TIP antibodies (Fig. 5 A, 2). As the seed matured (12–14 d after pollination), what appeared to be the translocation of DIP organelles into PSVs (Fig. 5 A, 3, open arrows) and their aggregation within PSVs (Fig. 5 A, 4, open triangles) were observed. These results indicate that DIP organelles originate in the cytoplasm in developing seeds, and that their localization inside seed PSVs is developmentally regulated. These observations would be consistent with those obtained in root tip cells (Fig. 3 A, 7 and 8).

The ultrastructure of DIP-positive structures in developing seeds provided clues as to their assembly. DIP labeling was observed over ~200 nm vesicles in the cytosol, some of which contained internal lucent areas (Fig. 5 B, 1). The crystalloid inside PSVs in developing seeds contained numerous lucent areas reminiscent of the appearance of multivesicular bodies (Robinson et al., 1998a) (Fig. 5 B, 2). Additionally, these structures appeared to be composed of subunits that were aggregated together because the linear patterns of the crystalloid were almost horizontal in one section (open arrow) and vertical (solid arrow) in another, with the two sections separated by a lucent junction (indicated by triangles). This type of organization has been reported for crystalloid in mature seeds from other species (Lott, 1980).

Biochemical Analysis of Purified Crystalloid

Our localization of the two integral membrane proteins, Re-F-B-α and DIP, in PSV crystalloid argued that crystalloids must contain lipid. To test this hypothesis directly, we purified PSVs and their crystalloids from pumpkin cotyledons. The PSV preparation (Fig. 6 A) was indistinguishable from the results obtained by Hara-Nishimura et al. (1982). However, we found that it was necessary to wash the crystalloid preparation through a second gradient to remove adherent contaminants. Additionally, we found that pumpkin crystalloids, in contrast to the results from castor beans (Tully and Beevers, 1976; Youle and

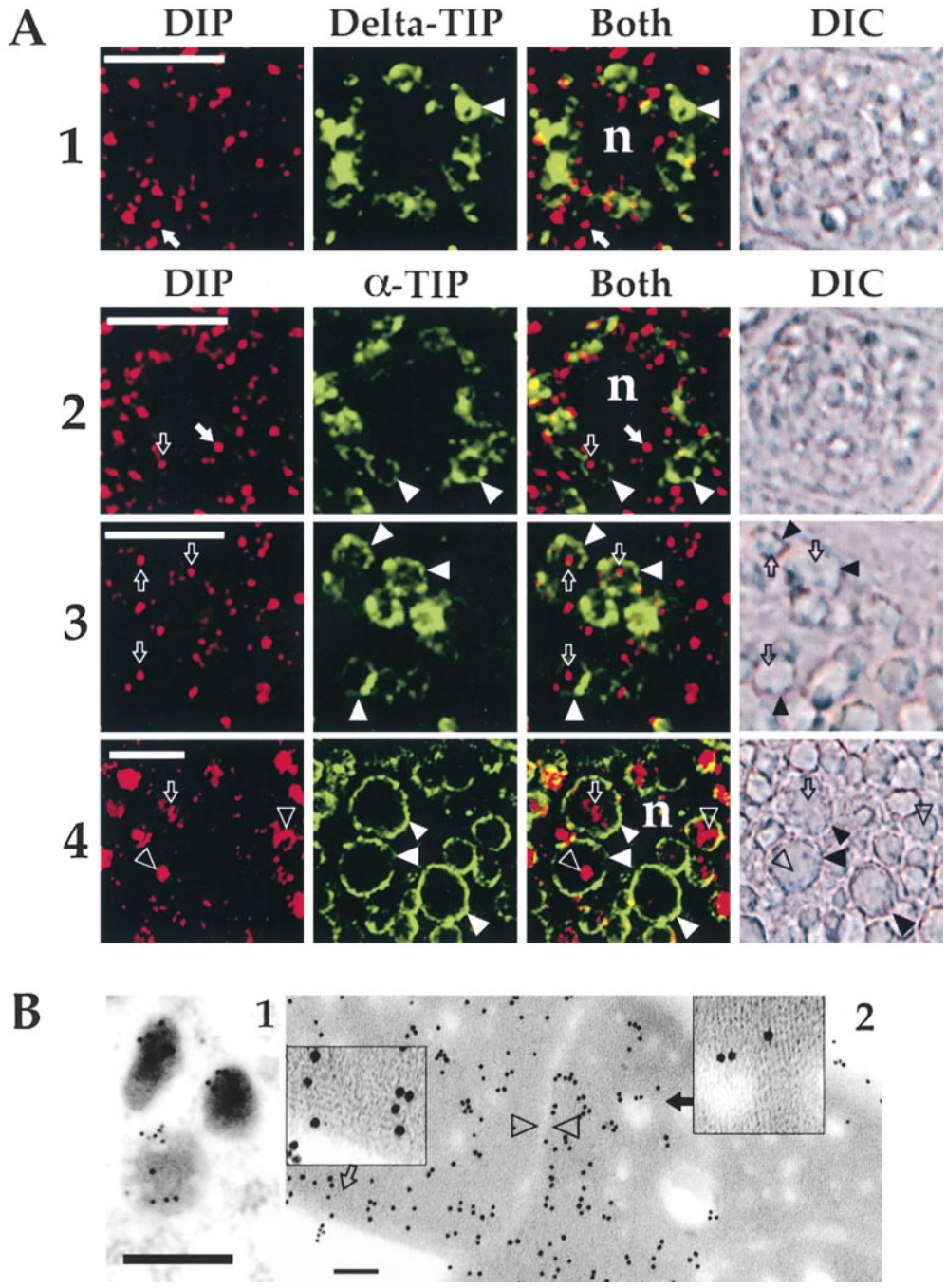

Figure 5. Association between DIP organelles and PSV compartments in developing tobacco seeds. (A) Paraffin-embedded sections prepared from immature seeds at 10 days after pollination (DAP; 1 and 2) and 12 DAP (2 and 3) were double-labeled with anti-DIP (red) and anti–δ-TIP (1, green) or anti–α-TIP (2, green) antibodies and visualized by confocal immunofluorescence. (1 and 2) Closed arrows indicate examples of an individual DIP compartment separated from PSVs (arrow heads); (2 and 3) DIP-containing organelles (open arrows) within PSVs (arrowheads). (4) Accumulation of multiple DIP-positive structures within PSV (open arrow) and appearance of larger DIP-positive structures (open arrowhead). Panels on the right present nonconfocal DIC images corresponding to those presented for immunofluorescence images. In 3 and 4, black arrowheads indicate PSVs corresponding to those indicated with closed arrowheads in immunofluorescence panels. Open symbols in DIC panels are provided as points of reference only. n, nucleus for all panels. (B) Immuno-EM localization of DIP in developing seeds (12 DAP). 1. Cytoplasmic vesicles labeled by anti-DIP antibodies. (2) Developing crystalloid within the vacuole lumen. Open and closed arrows indicate regions of the crystalloid (enlarged within the adjacent boxes) where the striations of the crystalloid lattice run almost horizontally and almost vertically, respectively. These two sections of the crystalloid are separated by a lucent strip (indicated between the two triangles). Bars: (A) 10 μm; (B, 1) 200 nm; (B, 2) 100 nm.

Huang, 1976), were not retained on an 80% sucrose cushion, but instead were pelleted to the bottom of the gradient; thus, our final crystalloid preparation (Fig. 6 B) also contained globoid crystals (Tully and Beevers, 1976; Youle and Huang, 1976). The protein profiles from SDS-PAGE analysis of the matrix (Fig. 6 C, lane 1), 30% sucrose surface (lane 2), 30–45% sucrose interface (lane 3), and 45–68% sucrose interface (lane 4) from the first gradient, and 68% sucrose surface (lane 5) and crystalloid pellet (lane 6) from the second gradient are shown in Fig. 6 C. Consistent with previous studies (Hara-Nishimura et al., 1982, 1998), the storage proteins p51 (asterisk) and globulin heavy (dot) and light (open circle) chains were abundant in all fractions including purified crystalloid (lane 6).

The specificity of the fractionation procedure was documented by comparing the distribution of DIP (Fig. 6 D, top) and δ-TIP (Fig. 6 D, bottom) in the various fractions. Very small amounts of DIP were detected in the protein from each sucrose step in gradient 1 (lanes 2–4), but >95% was present in approximately equal fractions on the

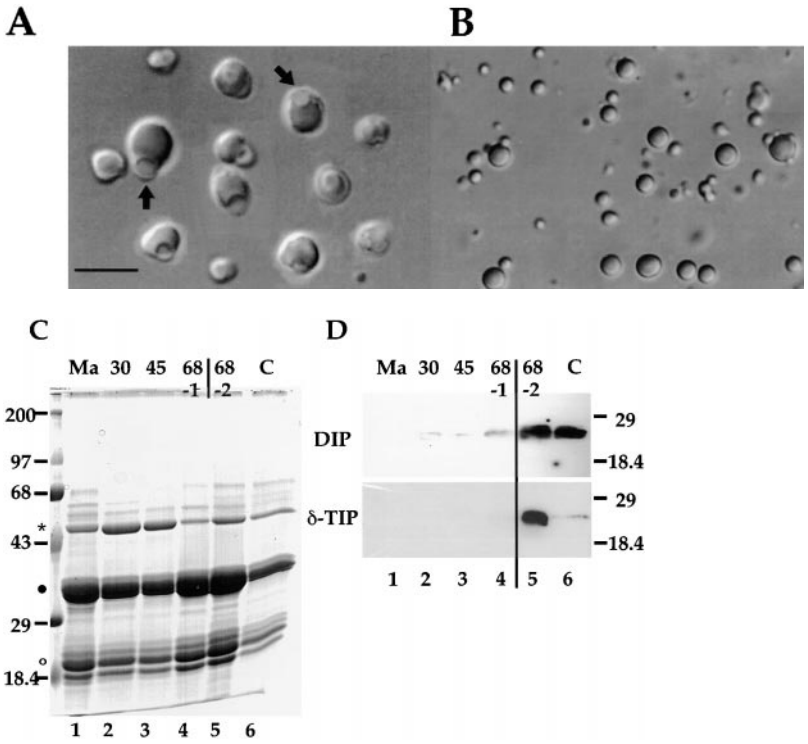

Figure 6. Purification of PSVs and crystalloids from pumpkin seeds. (A) Purified PSVs resuspended in glycerol; arrows indicate examples of crystalloids. (B) Purified crystalloids resuspended in 5 mM TE buffer. Bar, 20 μm. (C) Coomassie blue-stained SDS-PAGE gel: 100 μg of protein was electrophoresed from each fraction (lanes 1–6). Lane at far left contains molecular mass markers, with masses in kilodaltons indicated. Ma, matrix fraction (lane 1); 30, fraction from surface of 30% sucrose (lane 2); 45, 30–45% sucrose interface (lane 3); 68-1, 45–68% interface (lane 4); 68-2, fraction from 68% sucrose surface in second gradient (lane 5); and C, purified crystalloid (lane 6). Positions of p51 and globulin heavy and light chains are indicated with an asterisk, dot, and a circle, respectively. (D) Immunoblot analyses. Proteins from replicate gels, similar to that shown in C, were transferred to nitrocellulose and probed with anti-DIP (top) and anti–δ-TIP (bottom) antibodies. Positions of molecular mass markers are indicated to right; lane designations are same as in C.

68% sucrose cushion from the second gradient (lane 5) and in the crystalloid pellet (lane 6). In contrast, essentially all δ-TIP, a marker for PSV tonoplast, was present on the 68% sucrose cushion from the second gradient (lane 5), with very little associated with the crystalloid pellet (lane 6). This result indicated that the final crystalloid preparation had little contamination from adherent PSV tonoplast membrane. We determined the amount of lipid based on quantitation of the fatty acyl components relative to the amount of protein in the crystalloid preparation. In a sample representing 25% of the crystalloid preparation, there was 3.2 mg of protein and 0.85 mg of lipid (a wt/wt ratio of ~3.8:1). In contrast, 12 mg of protein and 0.7 mg of lipid (a ratio of 17:1) was measured in a sample representing half of the material collected at the surface of the 68% cushion. Considering that the crystalloid preparation contained substantial amounts of soluble storage proteins (see above), this result indicates a high concentration of lipid relative to potential integral membrane protein, and supports the concept that crystalloid contains lipid membranes.

RMR Proteins

We hypothesized that the 1–2-μm DIP organelles present in the cytoplasm of cells in root tips and developing seeds might serve as prevacuolar compartments for PSVs, and that the DIP-positive vesicles (Fig. 5 B, 1) might represent trafficking intermediates serving those compartments. If so, in addition to serving as the destination for Re-F-B-α that trafficked directly from the ER, the DIP organelles should also accumulate proteins trafficking from the Golgi apparatus. We have identified a receptor-like protein with those characteristics.

The vacuolar sorting receptor (VSR) proteins, of which BP-80 (Paris et al., 1997) is a prototype, are thought to function as sorting receptors in a Golgi to lytic vacuole pathway (Jiang and Rogers, 1998; Neuhaus and Rogers, 1998). The NH_2-terminal ~400 amino acids of these proteins define a unique region that was previously thought to lack homologues outside of the plant kingdom. Reexamination of the sequences of two unusual *Arabidopsis thaliana* EST cDNA clones previously identified in database homology searches using the unique VSR region as a query has, however, provided a different picture. Fig. 7 presents the derived amino acid sequences predicted from EST Z35151 and a cDNA (JR702) cloned in our laboratory using EST Z35151 as a probe, from a second cDNA (JR700) cloned using EST Z34589 as a probe, and from two *Arabidopsis* genomic clones, T22J18.16 and AC006567. At the NH_2 termini are typical signal peptide sequences (boxed), followed by a region homologous to VSR proteins, as shown by comparison to residues 77–139 of VSR_{At-2} (Paris et al., 1997). However, distinct from VSR proteins, beginning with position ~180 is a typical transmembrane domain (lower case) in Z35151/JR702, AC006567, T22J18.16, and JR700. All contain a typical RING-H2 domain as indicated by the asterisks and dots below the sequences. These predicted proteins end with serine-rich regions that lack apparent similarities other than paired Phe residues near their COOH termini (bold print). Z35151/JR702, AC006567, and T22J18.16 also share CT similarities (indicated in italics). The C-RZF protein, expressed in chicken embryo brain and heart cells (Tranque et al., 1996), shares with the plant sequences a signal peptide, VSR homology region, transmembrane sequence, RING-H2 domain, and a serine-rich COOH terminus. Its COOH terminus is also rich in acidic residues.

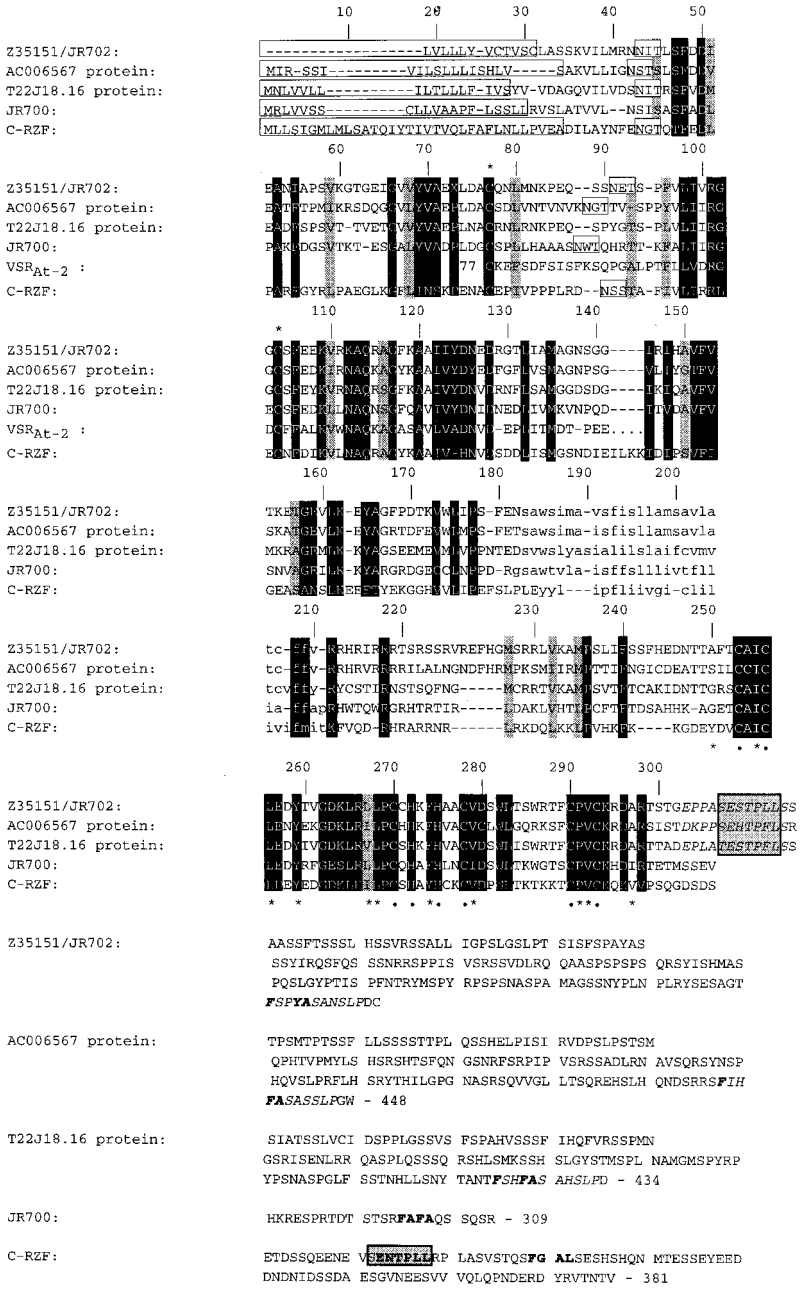

Figure 7. RMR proteins. Aligned are protein sequences derived from Z35151/JR702, from genomic sequences AC006567 and T22J18.16, from JR700, protein sequence corresponding to amino acids 77–139 from VSR$_{At-2}$ (clone MJ447 [Paris et al., 1997]; and the sequence of C-RZF [Tranque et al., 1996]). Numbers above the aligned sequences serve as reference points only. Z35151 is a partial length clone truncated at both 5′ and 3′ ends; JR702's 5′ truncation coincides with the alanine residue at position 76. These sequences are homologous as judged from smallest sum probability (P) scores obtained as follows using ungapped BLAST search comparisons (http://www.ncbi.nlm.nih.gov/blast/). When residues 77–138 from Z35151 were the query sequence, the corresponding sequence from Z34589 (JR700) gave $P = 6.1 \times 10^{-10}$ and C-RZF gave $P = 4 \times 10^{-5}$. When the same residues from VSR$_{At-2}$ were the query sequence, Z34589 gave $P = 0.00049$. Signal peptides predicted from PSORT (http://psort.nibb.ac.jp:8800) and from SignalP (http://www.cbs.dtu.dk/services/SignalP/) analyses are represented by rectangular boxes at the sequences' NH_2 termini. Internal boxed triplets indicate potential asparagine glycosylation sites. Residues identical at a given position in all, or all but one, of the aligned sequences are highlighted with black; similar residues at a given position in all of the sequences are highlighted with gray. The two asterisks above the sequences indicate two conserved cysteine residues that would be expected to form an intramolecular disulfide bond during chaperone-assisted folding in the ER. A transmembrane domain for each sequence predicted from TMpred (http://www.isrec.isb-sib.ch/software/TMPRED_form.html) and from PSORT analyses is indicated with lowercase letters. Beneath the alignments are dots and asterisks to indicate highly conserved RING H2 zinc binding ligands and hydrophobic residues (Saurin et al., 1996), respectively. In bold type are FXXFA or FXFA residues near the COOH termini of the plant sequences, while two clusters of sequence similarity in JR703, AC006567 and T22J18.16 COOH-terminal regions are italicized. In C-RZF, ENTPLL and FGAL in bold type indicate potential dileucine- and tyrosine-based targeting motifs, respectively. Gray boxes show conserved dileucine motif sequences in three plant proteins and C-RZF. Numbers at the ends of the sequences indicate the number of amino acid residues presented for each.

C-RZF and the plant proteins should all be Type I integral membrane proteins. We have designated these proteins as ReMembR-H2, or RMR, for receptor homology region-transmembrane domain-Ring H2 motif proteins.

An RMR Protein Colocalizes with DIP

To study the subcellular localization of an RMR protein, we prepared two antibodies, one raised against a recombinant protein corresponding to the lumenal portion (NT) of the Z35151/JR702 protein (residues 17–155), and the other against a synthetic peptide corresponding to residues 272–287 in its cytoplasmic tail (CT). As shown in Fig. 8 A, both antibodies (NT and CT) detected a single protein of the same, appropriate size on Western blots of *Arabidopsis* root extracts. These antibodies were used in immunofluorescence experiments to localize the protein. We used both *Arabidopsis* and tomato cells because the sequence of an RMR protein predicted from a tomato EST clone, AW223218, is very similar to that of the *Arabidopsis* pro-

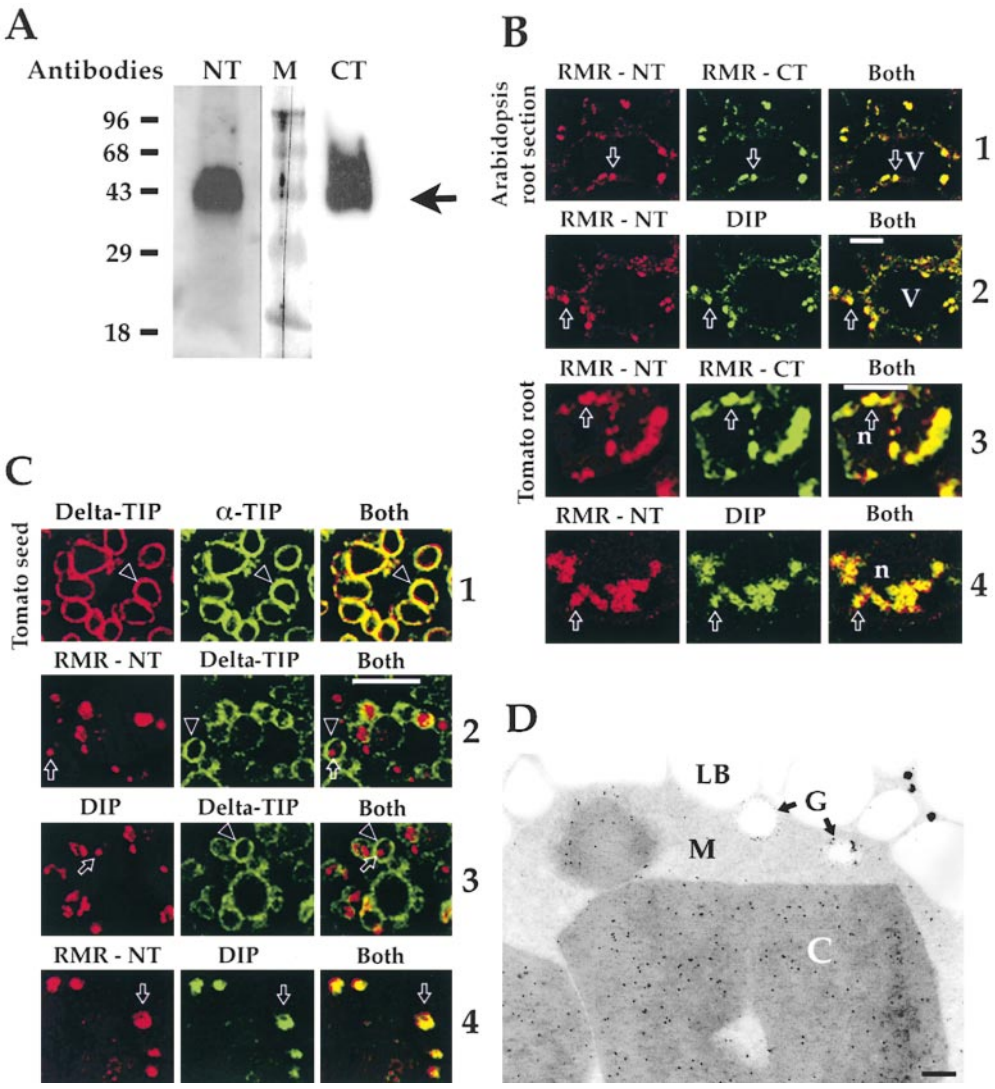

Figure 8. RMR protein and DIP colocalize. (A) Western blot detection of RMR protein from root extracts of *Arabidopsis*; arrow indicates RMR protein. Antibodies raised against the lumenal portion of RMR protein Z35151/JR702 (NT; residues 17–155) or to a synthetic peptide corresponding to 16 amino acids of its cytoplasmic tail (CT; residues 272–278) were used. M, molecular mass markers with sizes in kilodaltons indicated to the left. (B) RMR and DIP colocalize in root tip cells of *Arabidopsis* and tomato. Paraffin-embedded sections of *Arabidopsis* (1 and 2) and root tip cells of tomato (3 and 4) were double-labeled with two antibodies as indicated above each panel. Open arrows indicate examples of organelles where each pair of antibodies colocalizes. V, vacuole; n, nucleus. (C) RMR and DIP colocalize within PSVs in mature tomato seeds. Paraffin-embedded sections of mature tomato seeds were double-labeled with two antibodies as indicated above each panel. (1) Control to demonstrate that in tomato, as in tobacco, PSV tonoplast contains both α- and δ-TIPs (arrowhead). (2) Organelle labeled for RMR (red, arrow) is within PSV marked by δ-TIP (green, arrowhead). (3) Organelle labeled for DIP (arrow, red) is within PSV marked by δ-TIP (green, arrowhead). (4) RMR and DIP antibodies colocalize (arrow). Quantitation of the extent of colocalization for each pair of antibodies for relevant panels is presented in Table I. (D) Immuno-EM labeling of tomato PSV crystalloid (C) with a mixture of anti-RMR lumenal and cytoplasmic domain antibodies. M, matrix; LB, lipid body; G, globoid cavity. Bars, 200 nm.

tein, including a highly conserved region with a single glutamic to aspartic acid change corresponding to the peptide used for preparing the antibody.

As shown in Fig. 8 B (1 and 3), the NT and CT antibodies colocalized on the same organelles in *Arabidopsis* and tomato root cells, respectively. These organelles were also labeled with the anti-DIP antibodies (Fig. 8 B, 2 and 4, and Table I). The facts that the antibodies were highly specific (Fig. 8 A), and that both identified the same, DIP-positive organelles is strong evidence that these organelles contain the RMR protein in both plant species. When mature tomato seeds were studied, the pattern for RMR protein labeling (Fig. 8 C, 1) was indistinguishable from that for DIP (Fig. 8 C, 2), and the two antibodies colocalized when compared directly (Fig. 8 C, 3, and Table I). Electron microscopy immunocytochemistry confirmed that this labeling was indeed localized to PSV crystalloid (Fig. 8 D).

Use of a Reporter Protein to Determine Traffic of RMR Proteins in Tobacco Protoplasts

Our reporter protein system utilizes specific proteolytic processing of the proaleurain moiety as a marker for traffic to the lytic prevacuolar compartment (Jiang and Rogers, 1998). Thus, the proaleurain moiety in a reporter protein containing the BP-80 TMD/CT (designated Re-F-B-B) was processed into a mature form, whereas Re-F-B-α, with the α-TIP CT, was directed to a vacuolar compartment where processing did not occur (Jiang and Rogers, 1998). Therefore, we constructed a new reporter protein containing TMD/CT from the RMR protein JR702 designated Re-F-R-R (Fig. 9 A). When this protein was studied in pulse-chase immunoprecipitation experiments in tobacco protoplasts, the protein was present exclusively in the membrane fraction and remained intact throughout the 4-h chase period (Fig. 9 B). This pattern was similar to

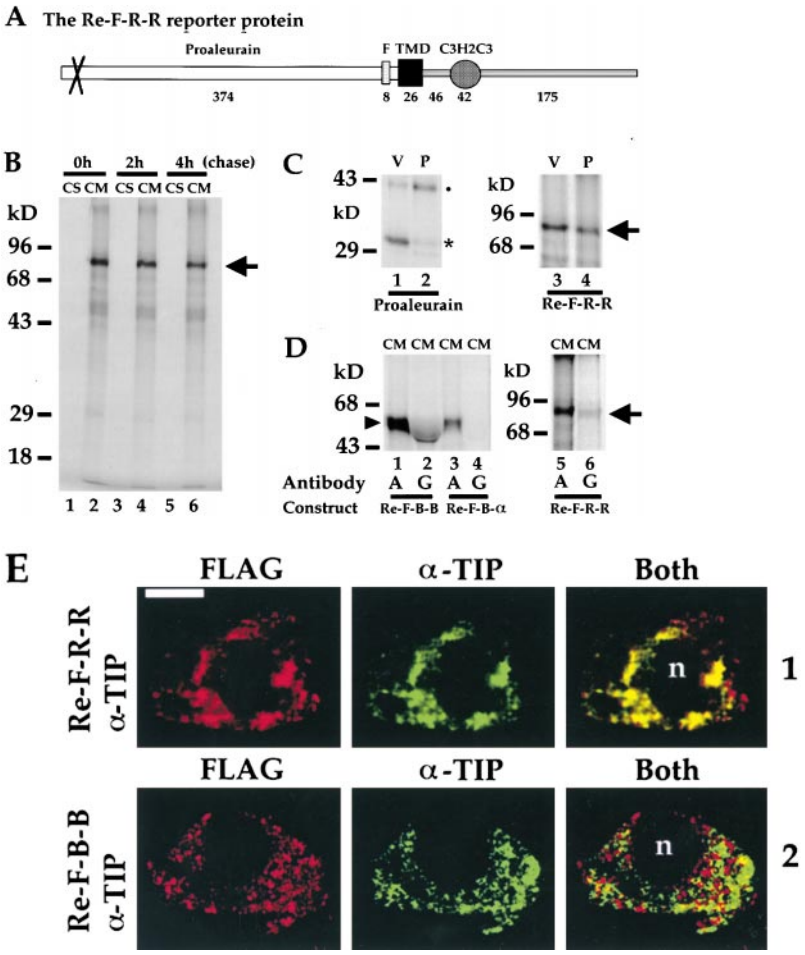

Figure 9. A reporter protein containing the RMR TMD and CT traffics via the Golgi apparatus to a PSV-like compartment in tobacco suspension culture cells. (A) Schematic illustration of the Re-F-R-R reporter protein that contains mutated proaleurain (open rectangle), the FLAG epitope (F, stippled rectangle), the transmembrane domain (TMD, black rectangle) and the RMR cytoplasmic tail (CT, gray with horizontal stripes). The RMR CT contains a RING-H2 motif (C3H2C3, stippled circle). The numbers below indicate the number of amino acid residues in each portion of the sequence. (B) Pulse-chase analysis of Re-F-R-R. Protoplasts expressing Re-F-R-R were labeled with [^{35}S]methionine and cysteine for 1 h and chased with cold methionine and cysteine for an additional 2 and 4 h before soluble (CS) and membrane (CM) fractions (Jiang and Rogers, 1998) were collected. Each sample was immunoprecipitated with antialeurain antibodies, followed by SDS-PAGE and fluorography. The arrow in B–D indicates the full-length Re-F-R-R reporter protein. (C) Re-F-R-R reaches vacuoles. Protoplasts expressing wild-type proaleurain (lanes 1 and 2) and Re-F-R-R (lanes 3 and 4) were labeled with [^{35}S]methionine and cysteine for 3 h before vacuole (V) and pellet (P) fractions were collected. Each sample was immunoprecipitated with antialeurain antibodies, followed by SDS-PAGE and fluorography. The dot and asterisk indicate proaleurain and mature aleurain, respectively. (D) Re-F-R-R acquires complex modifications to asparagine-linked glycans. Protoplasts expressing reporter proteins (Re-F-B-B, Re-F-B-α, and Re-F-R-R) were labeled with [^{35}S]methionine and cysteine for 3 h before CM fractions were collected. Each sample was immunoprecipitated by antialeurain antibodies (A, lanes 1, 3, and 5). Half of the immunoprecipitated products were reimmunoprecipitated with anti–complex glycan antibodies (G, lanes 2, 4, and 6), followed by SDS-PAGE and fluorography. The arrowhead indicates full-length Re-F-B-B and Re-F-B-α reporter proteins. (E) Re-F-R-R colocalizes with α-TIP protein when the two are coexpressed in tobacco protoplasts. Protoplasts coexpressing either Re-F-R-R/α-TIP (1) or Re-F-B-B/α-TIP (2) were fixed and double-labeled with anti-FLAG (red) and anti–α-TIP CT peptide (green) antibodies. n, nucleus. Bar, 10 μm.

that obtained previously with Re-F-B-α (Jiang and Rogers, 1998).

Although Re-F-R-R remained intact, it trafficked to a vacuolar compartment. We used a simple step gradient fractionation method after a 3-h labeling period to separate the ER and Golgi apparatus that collect in the pellet from vacuoles that float on the cushion (Jiang and Rogers, 1998). As shown for soluble proaleurain expressed in protoplasts as a positive control, the 42-kD precursor was predominantly in the pellet fraction (Fig. 9 C, lane 2, dot), whereas 32-kD–processed mature aleurain was predominantly in the vacuole fraction (lane 1, asterisk). More than half of intact Re-F-R-R partitioned in the vacuole fraction (Fig. 9 C, lane 3), a result similar to that obtained previously with Re-F-B-α (Jiang and Rogers, 1998).

Acquisition of complex modifications to asparagine-linked glycans as detected by anti–complex glycan antibodies is a marker for protein traffic through the plant Golgi apparatus (Jiang and Rogers, 1998). Therefore, we compared the glycosylation patterns of the three different reporter proteins. Consistent with previous results, antibodies against complex glycans detected the full-length protein from protoplasts expressing Re-F-B-B (Fig. 9 D, lane 2, arrowhead) but not Re-F-B-α (lane 4); this result was part of the basis for our conclusion that Re-F-B-α did not transit the Golgi apparatus on its way to a vacuole destination (Jiang and Rogers, 1998, 1999). In contrast, however, full-length Re-F-R-R was readily detected by anti–complex glycan antibodies (Fig. 9 D, lane 6, arrow). These results demonstrate that Re-F-R-R traffics through the Golgi apparatus before reaching a vacuolar compartment that lacks protease activity for processing the proaleurain moiety. The question remained, was it the same compartment to which Re-F-B-α moved?

We previously used colocalization with intact α-TIP protein to define the compartment to which Re-F-B-α moved when the two proteins were coexpressed (Jiang and Rogers, 1998). Therefore, we compared the localization of Re-F-R-R, detected with anti-FLAG, and α-TIP using double-labeled immunofluorescence in protoplasts coexpressing these two proteins. As shown in Fig. 9 E, 1, Re-F-R-R (red) and α-TIP protein (green), predominantly colocalized as indicated by the yellow color in the merged image (both). The extent of colocalization for anti-FLAG

and anti–α-TIP antibodies was 85 ± 18% (n = 12). In contrast, in protoplasts expressing Re-F-B-B, which traffics in the lytic vacuole pathway, and α-TIP (Fig. 9 E, 2), Re-F-B-B (red) and α-TIP (green) antibodies were largely separate, a result which is consistent with previous studies (Jiang and Rogers, 1998). This negative control supports the specificity of results with Re-F-R-R, which indicate that that reporter and the α-TIP protein were predominantly present in the same organelles when expressed together in tobacco protoplasts.

Discussion

In spite of substantial progress in identifying vesicle carriers for storage protein transport to PSVs in seeds (Hara-Nishimura et al., 1998; Hinz et al., 1999), relatively little is known of mechanisms for sorting proteins into the vesicles, of the identities and molecular composition of prevacuolar intermediates in the pathways, and of the relative contributions to these intermediates from pathways originating directly from the ER as compared with pathways from the Golgi apparatus. Additionally, the reasons why PSVs have a complex structure with morphologically distinct matrix, crystalloid, and globoid cavity compartments (Lott, 1980; Weber and Neumann, 1980) has been unexplained. Results presented here address some of these questions.

Our studies used antibodies against three different proteins, a chimeric reporter protein, Re-F-B-α, a fourth member of the tonoplast intrinsic protein family (Neuhaus and Rogers, 1998), DIP, and a novel receptor-like protein of the RMR family to define a new organelle in plant cells. We have shown that all three are concentrated in the PSV crystalloid and within 1–2-μm round and elongated structures in the cytoplasm of root tip cells and cells in the developing seed. We have designated these cytoplasmic structures as DIP organelles to emphasize the close correlation between the presence of different TIP isoforms and specific functions of organelles in the vacuolar system (Jauh et al., 1999). The presence of DIP in these organelles was defined by labeling with the anti-DIP peptide antibodies. We believe this definition is reliable because of the high specificity of the antibodies on Western blot analyses of tissue extracts and because we obtained essentially the same results using extracts and sections from three different plants: snapdragon, tomato, and tobacco. The presence of DIP within internal membranes rather than on a peripheral tonoplast further emphasizes the possibility of a structural function for the protein.

Further studies with DIP demonstrated that PSV crystalloid appears to be formed during seed development when 1–2-μm DIP organelles are taken up from the cytoplasm into PSVs where they aggregate to form the crystalloid. A similar uptake of DIP organelles into vacuoles in root tip cells also seems to be developmentally regulated. It is possible that this process may be related to the formation of what have been termed vacuolar protein bodies in vegetative tissues (Greyson and Mitchell, 1969; Shumway et al., 1972). As little or no DIP labeling was detected in the PSV tonoplast, and little or no labeling for δ-TIP or α-TIP (PSV tonoplast markers) was detected around or in the crystalloid, we hypothesize that the DIP organelles in the cytoplasm are surrounded by a membrane that fuses with the PSV tonoplast to deliver the internal, DIP-containing membranes to the vacuole interior.

This hypothesis is reasonable based upon precedents in other systems. The presence of distinct membrane domains, where the surrounding membrane and membrane comprising the internal multivesicular bodies have separate protein and lipid compositions, is well established for mammalian (Kobayashi et al., 1998) and yeast (Odorizzi et al., 1998) endosome/prevacuolar compartment multivesicular bodies. In the latter system, it is clear that the surrounding membrane fuses with the vacuole membrane to release the internal vesicles into the vacuole lumen where they are degraded (Odorizzi et al., 1998). In contrast, internal membranes from DIP organelles are preserved and form a distinct storage compartment in PSVs. Yolk platelets in oocytes represent endosomally derived multivesicular bodies that have been converted to a storage function, but there the yolk crystalloid is primarily formed from initially soluble yolk protein (Wall and Patel, 1987), whereas our results indicate that PSV crystalloid may receive its fundamental structure from membrane lamellae (see below).

The presence of Re-F-B-α indicates that the DIP organelles must be formed, in part, from membrane derived from the ER. The 15–amino acid α-TIP CT on Re-F-B-α was responsible for directing it to this destination. However, intact α-TIP was not present in DIP organelles, but rather was localized to PSV tonoplast. This observation indicates that multiple determinants for targeting must be present within an intact TIP molecule, a possibility that may explain different targeting results when green fluorescent protein was inserted at different positions in a γ-TIP protein sequence (Neuhaus, 2000). The facts that the RMR protein was also concentrated in DIP organelles, and that a reporter protein constructed with the RMR transmembrane domain and cytoplasmic tail moved through the Golgi apparatus before reaching the same vacuolar destination as that targeted by Re-F-B-α in tobacco protoplasts, argue that DIP organelles must also be the destination of vesicular traffic from the Golgi apparatus. Our chimeric reporter protein trafficking assay is based upon extensive precedents in both mammalian and yeast systems (Jiang and Rogers, 1998) that document the usefulness of the approach. However, we cannot exclude the possibility that interactions by the lumenal portion of an intact RMR protein might somehow modify traffic of the protein in a manner that could not be predicted from our assay. With this caveat in mind, our results indicate that DIP organelles serve as a Golgi to PSV prevacuolar compartment, but several questions remain to be answered about that function. It is not clear if all proteins destined for the PSV, including those destined for the matrix, move through DIP organelles. Their relationship to other organelles associated with the PSV pathway also remains to be established.

Because PSVs of legumes, including the pea, lack crystalloid, it is not clear how our results relate to those from studies that identified multivesicular bodies as prevacuolar organelles in developing pea cotyledons (Robinson et al., 1998a). Additionally, further studies will be necessary to relate our results to those obtained in cereal endosperm cells (Levanony et al., 1992; Herman and Larkins, 1999). However, it is likely that our results are relevant to the

pioneering studies of precursor-accumulating vesicles (Hara-Nishimura et al., 1991, 1998; Hayashi et al., 1999). Those studies used plants whose PSVs are known to contain crystalloid. The precursor-accumulating vesicles were shown to contain precursor forms of the pumpkin storage globulins (Hara-Nishimura et al., 1991, 1998), which are proteolytically processed to a mature form upon reaching the PSV (Hara-Nishimura and Nishamura, 1987; Hara-Nishimura et al., 1991). Thus, they clearly represent intermediates in a pathway to the PSV, and data strongly indicate that they initially form by budding directly from the ER (Hara-Nishimura et al., 1998; Hayashi et al., 1999). Additionally, precursor-accumulating vesicles also have functional and morphological characteristics of prevacuolar compartments that participate in Golgi to PSV traffic. In castor bean, proteins carrying Golgi-mediated complex modifications to asparagine-linked oligosaccharides are localized to the vesicles' peripheral lucent zone, whereas storage globulin precursors are predominantly localized to the central osmiophilic region (Hara-Nishimura et al., 1998). Interestingly, when purified precursor-accumulating vesicles were fixed and stained to optimize visualization of membranes, their peripheral lucent zone was shown to contain abundant internal vesicles (Hara-Nishimura et al., 1998). Thus, they represent a type of multivesicular body. It will be of some interest in the future to determine if they also contain DIP and RMR proteins. It is likely that the cytoplasmic and intravacuolar protein bodies containing zeins in the developing seeds of transgenic tobacco plants identified by Coleman et al. (1996) are equivalent to precursor-accumulating vesicles/DIP organelles.

The first RMR protein to be identified, C-RZF, was proposed to be a transcription factor localized to the nucleus (Tranque et al., 1996). However, those studies used antibodies directed to a sequence including the RING-H2 domain and may have cross-reacted with other nuclear proteins. In experiments using the antibodies to immunoprecipitate C-RZF, membrane fractions from the cells were not analyzed, and immunofluorescence patterns were consistent with both nuclear and endosomal labeling (Tranque et al., 1996). Thus, consistent with our analysis of the structure of C-RZF (Fig. 7), and our studies of the closely related plant RMR protein presented here, C-RZF and its mammalian equivalents may also be integral membrane proteins that traffic in an endosomal pathway. Although there is a more distantly related RMR protein predicted from a *Schizosaccharomyces pombe* genomic sequence (GenBank accession No. CAB0867.1), we have been unsuccessful in detecting homologues in the *Saccharomyces cerevisiae* genome. The lumenal domain of the RMR proteins is homologous to a portion of the BP-80 VSR protein that is known to participate in ligand binding (Cao et al., 2000). This raises the interesting possibility that RMR proteins could participate in protein–protein interactions during their transit through the Golgi apparatus. The question of whether these proteins could have a role in the sorting of soluble proteins to the plant PSV, or in a non-mannose-6-phosphate–mediated lysosomal sorting in mammalian cells (Glickman and Kornfeld, 1993; McIntyre and Erickson, 1993) remains to be investigated. The fact that the plant RMR protein was concentrated in the DIP organelles and PSV crystalloid indicates, however, that it may not recycle to the Golgi apparatus and that it may have a structural role in those locations.

The presence of a RING-H2 motif in the RMR cytoplasmic tail provides an additional mechanism for protein–protein interactions. Although this motif consists of two tandemly repeated sets of four zinc-binding ligands that interact with two zinc molecules in a unique cross-brace structure (Saurin et al., 1996) similar to that of the FYVE finger, the latter is distinguished by eight cysteine residues and by the presence of a cluster of highly conserved basic amino acids that are essential for its function (Gaullier et al., 1998; Misra and Hurley, 1999). Thus, the RING-H2 and FYVE fingers are structurally and functionally distinct. The RING-H2 motif is characteristically present at the COOH terminus of proteins that may interact on the cytoplasmic face of membranes. For example, rapsyn associates with the cytoplasmic portion of the acetylcholine receptor, where its RING-H2 domain is essential for receptor clustering (Bezakova and Bloch, 1998). In yeast, Vps18p/PEP3p and Vps11p/Pep5p are components of a protein complex that is associated with the vacuole membrane and is essential for the traffic of proteins to the vacuole (Rieder and Emr, 1997). A number of *Arabidopsis* integral membrane proteins with cytoplasmic RING-H2 motifs have been identified (Jensen et al., 1998), but these differ from RMR proteins in that they have little or no sequence at the NH_2 terminus that projects beyond the transmembrane domain, and they lack other conserved motifs identified in the cytoplasmic tails of the RMR proteins.

The presence of three integral membrane proteins in PSV crystalloid, Re-F-B-α, DIP, and the RMR protein, and the presence of substantial amounts of lipid in purified pumpkin crystalloid argue strongly that membranes comprise part of the crystalloid structure. This hypothesis would be consistent with the multilamellar structure of crystalloid as defined from freeze-fracture studies (Lott, 1980; Spitzer and Lott, 1980). Thus, we would predict that the lamellae are formed from parallel arrays of membranes separated by selected soluble proteins packaged between them. It will be of some interest to identify other protein components within the crystalloid and to define its lipid components. The knowledge that RING-H2 motifs are important in other systems for promoting protein–protein interactions would raise the possibility that RMR protein RING-H2–mediated interactions may help form or stabilize the crystalloid structure. The membrane surrounding the globoid cavity in PSVs carries a protein marker not present on either PSV tonoplast or crystalloid (Jiang, L., and J.C. Rogers, unpublished data). Thus, the PSV tonoplast, the crystalloid, and the globoid cavity each appear to derive from separate membrane-bound compartments and assemble during seed maturation into the final, compound organelle representing the mature PSV. It is likely that this unique structure is necessary for both optimal storage of proteins as well as for packaging of the machinery, which will later be rapidly activated during germination to digest the stored components.

We thank Drs. Frederick Meins and Chris Hawes for providing antibodies, and Dr. John Browse for performing lipid assays. The advice and assistance from Drs. Vince Franceschi and Chris Davitt at the microscopy center of Washington State University is greatly appreciated.

This research was supported by grants from the Department of En-

ergy (DE-FG03-97ER20277) and National Science Foundation (MCB-9974429) to J.C. Rogers.

Submitted: 19 January 2000
Revised: 28 June 2000
Accepted: 28 June 2000

References

Bezakova, G., and R.J. Bloch. 1998. The zinc finger domain of the 43-kDa receptor-associated protein, rapsyn: role in acetylcholine receptor clustering. *Mol. Cell. Neurosci.* 11:274–288.

Bradford, M. 1976. A rapid and sensitive method for the quantitation of microgram quantities of protein utilizing the principle of protein dye-binding. *Anal. Biochem*. 72:248–254.

Browse, J., P.J. McCourt, and C.R. Summerville. 1986. Fatty acid composition of leaf lipids determined after combined digestion and fatty acid methyl ester formation from fresh tissue. *Anal. Biochem*. 152:141–145.

Cao, X., S.W. Rogers, J. Butler, L. Beevers, and J.C. Rogers. 2000. Structural requirements for ligand binding by a plant vacuolar sorting receptor. *Plant Cell*. 12:493–506.

Coleman, C.E., E.M. Herman, K. Takasaki, and B.A. Larkins. 1996. The maize γ-zein sequesters α-zein and stabilizes its accumulation in protein bodies of transgenic tobacco endosperm. *Plant Cell*. 8:2335–2345.

Culianez-Macia, F.A., and C. Martin. 1993. DIP: a member of the MIP family of membrane proteins that is expressed in mature seeds and dark-grown seedlings of *Antirrhinum majus*. *Plant J.* 4:717–725.

Fitchette, A.-C., M. Cabanes-Macheteau, L. Marvin, B. Martin, B. Satiat-Jeunemaitre, V. Gomord, K. Crooks, P. Lerouge, L. Faye, and C. Hawes. 1999. Biosynthesis and immunolocaization of Lewis a-containing N-glycans in the plant cell. *Plant Physiol.* 121:333–343.

Frigerio, L., M. de Virgilio, A. Prada, F. Faoro, and A. Vitale. 1998. Sorting of phaseolin to the vacuole is saturable and requires a short C-terminal peptide. *Plant Cell*. 10:1031–1042.

Gaullier, J.-M., A. Simonsen, A. D'Arrigo, B. Bremnes, H. Stenmark, and R. Aasland. 1998. FYVE fingers bind PtdIns(3)P. *Nature*. 394:432–433.

Glickman, J.N., and S. Kornfeld. 1993. Mannose 6-phosphate-independent targeting of lysosomal enzymes in I-cell disease B lymphoblasts. *J. Cell Biol.* 123:99–108.

Greenwood, J.S., and M.J. Chrispeels. 1985. Correct targeting of the bean storage protein phaseolin in the seeds of transformed tobacco. *Plant Physiol.* 79: 65–71.

Greyson, R.I., and K.R. Mitchell. 1969. Light and electron microscope observations of a vacuolar structure associated with the floral apex of *Nigella damascena*. *Can. J. Bot.* 47:597–601.

Hara-Nishimura, I., and M. Nishamura. 1987. Proglobulin processing enzyme in vacuoles isolated from developing pumpkin cotyledons. *Plant Physiol.* 85: 440–445.

Hara-Nishimura, H., M. Nishimura, H. Matsubara, and T. Adazawa. 1982. Suborganellar localization of proteinase catalyzing the limited hydrolysis of pumpkin globulin. *Plant Physiol.* 70:688–703.

Hara-Nishimura, I., K. Inoue, and M. Nishimura. 1991. A unique vacuolar processing enzyme responsible for conversion of several precursors into mature forms. *FEBS (Fed. Eur. Biochem. Soc.) Lett.* 294:89–93.

Hara-Nishimura, I., T. Shimada, K. Hatano, Y. Takeuchi, and M. Nishimura. 1998. Transport of storage proteins to protein storage vacuoles is mediated by large precursor-accumulating vesicles. *Plant Cell*. 10:825–836.

Hayashi, M., K. Toriyama, M. Kondo, I. Hara-Nishimura, and M. Nishimura. 1999. Accumulation of a fusion protein containing 2S albumin induces novel vesicles in vegetative cells of *Arabidopsis*. *Plant Cell Physiol.* 40:263–272.

Herman, E.M., and B.A. Larkins. 1999. Protein storage bodies and vacuoles. *Plant Cell*. 11:601–613.

Hinz, G., S. Hillmer, M. Bäumer, and I. Hohl. 1999. Vacuolar storage proteins and the putative sorting receptor BP-80 exit the Golgi apparatus of developing pea cotyledons in different transport vesicles. *Plant Cell*. 11:1509–1524.

Hoffman, L.M., D.D. Donaldson, R. Bookland, K. Rashka, and E.M. Herman. 1987. Synthesis and protein deposition of maize 15-kD zein in transgenic tobacco seeds. *EMBO (Eur. Mol. Biol. Organ.) J.* 6:3213–3221.

Hoh, B., G. Hinz, B.-K. Jeong, and D.G. Robinson. 1995. Protein storage vacuoles form de novo during pea cotyledon development. *J. Cell Sci.* 108:299–310.

Inoue, K., A. Motozaki, Y. Takeuchi, M. Nishimura, and K. Hara-Nishimura. 1995. Molecular characterization of proteins in protein-body membrane that disappear most rapidly during transformation of protein bodies into vacuoles. *Plant J.* 7:235–243.

Jauh, G.-Y., A.M. Fischer, H.D. Grimes, C.A. Ryan, and J.C. Rogers. 1998. δ-Tonoplast intrinsic protein defines unique plant vacuole functions. *Proc. Natl. Acad. Sci. USA*. 95:12995–12999.

Jauh, G.-Y., T. Phillips, and J.C. Rogers. 1999. Tonoplast intrinsic protein isoforms as markers for vacuole functions. *Plant Cell*. 11:1867–1882.

Jefferson, R.A., T.A. Kavanaugh, and M.W. Bevan. 1987. GUS fusions: beta-glucuronidase as a sensitive and versatile gene fusion marker in higher plants. *EMBO (Eur. Mol. Biol. Organ.) J.* 6:3901–3907.

Jensen, R.B., K.L. Jensen, H.M. Jespersen, and K. Skriver. 1998. Widespread occurrence of a highly conserved RING-H2 zinc finger motif in the model plant *Arabidopsis thaliana*. *FEBS (Fed. Eur. Biochem. Soc.) Lett.* 436:283–287.

Jiang, L., and J.C. Rogers. 1998. Integral membrane protein sorting to vacuoles in plant cells: evidence for two pathways. *J. Cell Biol.* 143:1183–1199.

Jiang, L., and J.C. Rogers. 1999. Functional analysis of a Golgi-localized Kex2p-like protease in tobacco suspension culture cells. *Plant J.* 18:23–32.

Jiang, L., W.L. Downing, C.L. Baszczynski, and A.R. Kermode. 1995. The 5′ flanking regions of vicilin and napin storage protein genes are down-regulated by desiccation in transgenic tobacco. *Plant Physiol.* 107:1439–1449.

Kirsch, T., N. Paris, J.M. Butler, L. Beevers, and J.C. Rogers. 1994. Purification and initial characterization of a potential plant vacuolar targeting receptor. *Proc Natl. Acad. Sci. USA*. 91:3403–3407.

Kobayashi, T., E. Stang, K.S. Fang, P. de Moerloose, R.G. Parton, and J. Gruenberg. 1998. A lipid associated with the antiphospholipid syndrome regulates endosome structure and function. *Nature*. 392:193–197.

Levanony, H., R. Rubin, Y. Altschuler, and G. Galili. 1992. Evidence for a novel route of wheat storage proteins to vacuoles. *J. Cell Biol.* 119:1117–1128.

Lott, J.N.A. 1980. Protein bodies. *In* The Biochemistry of Plants. Vol. 1. N.E. Tolbert, editor. Academic Press, New York. 589–623.

McIntyre, G.F., and A.H. Erickson. 1993. The lysosomal proenzyme receptor that binds procathepsin L to microsomal membranes at pH 5 is a 43-kDa integral membrane protein. *Proc. Natl. Acad. Sci. USA*. 90:10588–10592.

Misra, S., and J.H. Hurley. 1999. Crystal structure of a phosphatidylinositol 3-phosphate-specific membrane-targeting motif, the FYVE domain of Vps27p. *Cell*. 97:657–666.

Müntz, K. 1998. Deposition of storage proteins. *Plant Mol. Biol.* 38:77–99.

Næsted, H., G.I. Frandsen, G.-Y. Jauh, I. Hernandez-Pinzon, H.B. Nielsen, D. Murphy, J.C. Rogers, and J. Mundy. 2000. Caleosins: Ca^{2+} binding proteins associated with oil-bodies. *Plant Mol. Biol.* In press.

Neuhaus, J.-M. 2000. GFP as a marker for vacuoles in plants. *Annu. Plant Rev.* In press.

Neuhaus, J.M., M. Pietrzak, and T. Boller. 1994. Mutation analysis of the C-terminal vacuolar targeting peptide of tobacco chitinase: low specificity of the sorting system, and gradual transition between intracellular retention and secretion into the extracellular space. *Plant J.* 5:45–54.

Neuhaus, J.M., and J.C. Rogers. 1998. Sorting of proteins to vacuoles in plant cells. *Plant Mol. Biol.* 38:127–144.

Odorizzi, G., M. Babst, and S.D. Emr. 1998. Fab1p PtdIns(3)P 5-kinase function essential for protein sorting in the multivesicular body. *Cell*. 95:847–858.

Okita, T.W., and J.C. Rogers. 1996. Compartmentation of proteins in the endomembrane system of plant cells. *Annu. Rev. Plant Physiol. Plant Mol. Biol.* 47:327–350.

Paris, N., C.M. Stanley, R.L. Jones, and J.C. Rogers. 1996. Plant cells contain two functionally distinct vacuolar compartments. *Cell*. 85:563–572.

Paris, N., S.W. Rogers, L. Jiang, T. Kirsch, L. Beevers, T.E. Phillips, and J.C. Rogers. 1997. Molecular cloning and further characterization of a probable plant vacuolar sorting receptor. *Plant Physiol.* 115:29–39.

Rieder, S.E., and S.D. Emr. 1997. A novel RING finger protein complex essential for a late step in protein transport to the yeast vacuole. *Mol. Biol. Cell*. 8:2307–2327.

Robinson, D.G., M. Bäumer, G. Hinz, and I. Hohl. 1998a. Vesicle transfer of storage proteins to the vacuole: the role of the Golgi apparatus and multivesicular bodies. *J. Plant Physiol.* 152:659–667.

Robinson, D.G., G. Galili, E. Herman, and S. Hillmer. 1998b. Topical aspects of vacuolar protein transport: autophagy and prevacuolar compartments. *J. Exp. Bot.* 49:1263–1270.

Rogers, S.W., M. Burks, and J.C. Rogers. 1997. Monoclonal antibodies to barley aleurain and homologues from other plants. *Plant J.* 11:1359–1368.

Saurin, A.J., K.L.B. Borden, M.N. Boddy, and P.S. Freemont. 1996. Does this have a familiar RING? *Trends Biochem. Sci.* 21:208–214.

Shumway, L.K., V. Cheng, and C.A. Ryan. 1972. Vacuolar protein in apical and flower-petal cells. *Planta*. 106:279–290.

Spitzer, E., and J.N.A. Lott. 1980. Thin–section, freeze-fracture, and energy dispersive x-ray analysis studies of the protein bodies of tomato seeds. *Can. J. Bot.* 58:699–711.

Sturm, A., and M.J. Chrispeels. 1988. Correct glycosylation, Golgi-processing, and targeting to protein bodies of the vacuolar protein phytohemagglutinin in transgenic tobacco. *Planta*. 175:170–183.

Tranque, P., K.L. Crossin, C. Cirelli, G.M. Edelman, and V.P. Mauro. 1996. Identification and characterization of a RING zinc finger gene (C-RZF) expressed in chicken embryo cells. *Proc. Natl. Acad. Sci. USA*. 93:3105–3109.

Tully, R.E., and H. Beevers. 1976. Protein bodies of castor bean endosperm. *Plant Physiol.* 58:710–716.

Wall, D.A., and S. Patel. 1987. Multivesicular bodies play a key role in vitellogenin endocytosis by *Xenopus* oocytes. *Dev. Biol.* 119:275–289.

Weber, E., and D. Neumann. 1980. Protein bodies, storage organelles in plant seeds. *Biochem. Physiol. Pflanzen*. 175:279–306.

Yamamoto, Y.T., C.G. Taylor, G.N. Acedo, C.-L. Cheng, and M.A. Conkling. 1991. Characterization of *cis*-acting sequences regulating root-specific gene expression in tobacco. *Plant Cell*. 3:371–382.

Youle, R.J., and A.H.C. Huang. 1976. Protein bodies from the endosperm of castor bean. *Plant Physiol.* 58:703–709.